

Letter to the Editor

Discovery of solid HDO in grain mantles[★]

T.C. Teixeira¹, J.P. Devlin², V. Buch³, and J.P. Emerson⁴

¹ Institute of Physics and Astronomy, University of Århus, Ny Munkegade, DK-8000 Århus C, Denmark (tct@obs.aau.dk)

² Department of Chemistry, Oklahoma State University, USA (devlin@osuunx.ucc.okstate.edu)

³ Department of Physical Chemistry, Hebrew University of Jerusalem, Israel (viki@fh.huji.ac.il)

⁴ Department of Physics, Queen Mary and Westfield College, Mile End Road, London E1 4NS, UK (j.p.emerson@qmw.ac.uk)

Received 5 May 1999 / Accepted 10 June 1999

Abstract. The observation of deuterium fractionation in the molecular gas in hot cores is currently interpreted as evaporation of deuterium-rich molecules from the icy grain mantles where they accumulated during the cold, dense cloud core stage. The predicted enrichment in deuterium of the ices has never been observed. This work provides the first detections of solid HDO in grain mantles. We find column densities in the solid state of $N_s(\text{HDO}) = (3.23 \pm 0.03) \times 10^{16} \text{ cm}^{-2}$ for W33A, and $N_s(\text{HDO}) = (7.78 \pm 0.03) \times 10^{16} \text{ cm}^{-2}$ for NGC7538 IRS9. The estimated $[\text{HDO}]/[\text{H}_2\text{O}]$ ratios range from 8×10^{-4} in W33A to 10^{-2} in NGC7538 IRS9. These values are comparable to the predictions by chemical models, and provide support for the assumption that the origin of the deuterium enhancement in “hot cores” is evaporation from grain mantles.

Key words: line: identification – ISM: dust, extinction – ISM: molecules – infrared: ISM: lines and bands

1. Introduction

Observations of deuterated molecules in the gas phase towards cold clouds (TMC-1), warm clouds and “hot cores” have shown significant fractionation effects (e.g. Millar & Hatchell 1998 and references therein). In particular, in “hot cores” the abundances of deuterated species can reach factors of ~ 100 to ~ 1000 larger than those expected on the basis of the cosmic $[\text{D}]/[\text{H}]$ ratio of 1.6×10^{-5} (Dring et al. 1997). The detection of such high abundances of deuterated molecules in “hot cores” is surprising, as it is difficult to produce and maintain deuterium enrichment through gas-phase chemistry at the high temperatures ($T \gtrsim 100 \text{ K}$) of those regions (Millar et al. 1989; Jacq et al. 1990; Rodgers & Millar 1996). The current interpretation of this deuteration enhancement in “hot cores” involves gas-grain

chemistry during the cold, dense cloud core stage, followed by evaporation from the grain mantles of the deuterated molecules when a star is formed at the centre of the core (e.g. Millar & Hatchell 1998), or by the passage of a shock (Bergin et al. 1999).

The importance of reactions involving deuterium in grain mantles for the enhancement of the abundance of deuterated molecules, was originally noted by Tielens (1983). Brown & Millar (1989) produced time-dependent chemical models of a dense quiescent cloud and of a “hot core”, including deuterium-bearing species and accretion onto the grains. These models produced a high abundance of deuterated molecules in the grain mantles during the cold, dense cloud stage, which is reflected in the expected enhanced fractionation of deuterated species by evaporation during the “hot core” phase.

Presently, the enrichment in deuterium of the icy mantles, although predicted by theoretical models, has not been observed. The origin of the high levels of fractionation of deuterated gaseous species in “hot cores” is therefore still only a supposition. The observation of deuterated species in the grain mantles would be the first demonstration that mantle chemistry in fact generates deuterium enrichment, and a crucial test for the models of cloud chemistry.

Water-ice has been shown to be ubiquitous in grain mantles: H_2O is by far the most abundant molecule in the icy mantles, with an abundance comparable to that of gaseous CO (Tielens et al. 1991). Taking the models of Tielens (1983) and Brown & Millar (1989), the estimated abundance of HDO in the mantles is of the order of 1% and 6%, respectively, of the abundance of H_2O -ice at the densities characteristic of dense cloud cores. The infrared feature due to OD stretch of HDO in amorphous H_2O ice deposits produces a broad absorption around 2450 cm^{-1} ($4.1 \mu\text{m}$) (Mayer & Pletzer 1985) which is inaccessible from the ground but accessible to the Infrared Space Observatory (ISO, Kessler et al. 1996). Because of the high abundance of water-ice in grain mantles and of the infrared spectrum of HDO, this species is the best candidate for the detection of deuterated molecules in the solid state in molecular clouds. Its detection may provide the missing link between theory and observations in dark cloud chemistry.

Send offprint requests to: T.C. Teixeira

[★] Based on observations with ISO, an ESA project with instruments funded by ESA Member States (especially the PI countries: France, Germany, the Netherlands and the United Kingdom) and with the participation of ISAS and NASA.

2. Observations

The ISO short wavelength spectrometer (SWS; de Graauw et al. 1996a) was used in grating mode AOT06. Spectra were obtained from $3.621\ \mu\text{m}$ to $4.527\ \mu\text{m}$. For point sources, the mean resolving power of the instrument in this mode and wavelength range is $\lambda/\Delta\lambda \sim 2000$. The target sources – W33A ($\alpha_{2000} = 18^{\text{h}}14^{\text{m}}39^{\text{s}}.0$, $\delta_{2000} = -17^{\circ}52'04''$), NGC7538 IRS9 ($\alpha_{2000} = 18^{\text{h}}22^{\text{m}}26^{\text{s}}.2$, $\delta_{2000} = -13^{\circ}30'08''$), and AFGL2136 ($\alpha_{2000} = 23^{\text{h}}14^{\text{m}}01^{\text{s}}.6$, $\delta_{2000} = 61^{\circ}27'20''$) – were chosen primarily for the large column density of water-ice in their lines-of-sight. Each spectrum was taken in four segments: $[3.621, 3.880]\ \mu\text{m}$, $[3.831, 4.060]\ \mu\text{m}$, $[4.039, 4.310]\ \mu\text{m}$, and $[4.260, 4.528]\ \mu\text{m}$. Data reduction was carried out in August 1998, using the ISO SWS Interactive Analysis System. The data processing departed from the pipeline at the Standard Processed Data stage, and all subsequent processing was done interactively. Once each of the segments was processed, the ISO Spectral Analysis Package was used for further processing. To produce continuous spectra, the segments of each spectrum were “stitched” together by applying small shifts of typically less than 5% of the continuum level (with the exception of W33A, where a shift of 15% was applied to the first two segments), so that the overlapping regions matched. “Stitching” the spectra at $\sim 4.05\ \mu\text{m}$ was the most critical operation: the shifts were carefully chosen so that the Br α line present in each spectrum at $\sim 4.052\ \mu\text{m}$ matched in the two corresponding overlapping segments for each spectrum. Finally, the spectra were Hanning smoothed to a resolution of $\lambda/\Delta\lambda \sim 2000$.

3. The spectra

The resulting spectra, in Jansky, are presented in the left-hand side panels in Fig. 1. To determine the continuum for conversion of the spectra into optical depth units, a quadratic fit was performed to regions in the spectra selected to avoid features (possibly) present in the spectra, using χ^2 -minimization. The selected regions for the continuum are indicated at the top of each of the left-hand panels of Fig. 1. Other fits were attempted using higher level polynomials and other regions for the continuum, but those shown in the figure are the ones that appeared to fit the continuum best. While the continuum fits produce reasonable overall results, their performance is not completely satisfactory at the edges of the spectra. That is most noticeable in the spectrum of W33A and may be ascribed to three problems. First, the signal-to-noise ratio decreases toward the short-wavelength edge of the spectra, in particular for W33A and NGC7538 IRS9. Second, the long-wavelength edge of the spectrum of W33A might be affected by the deep $\sim 4.62\ \mu\text{m}$ XCN feature which is very prominent in the spectrum of that object (Lacy et al. 1984). Finally, the three spectra might be affected by a weak, broad (FWHM $\sim 200\ \text{cm}^{-1}$) absorption band of water-ice at $\sim 4.5\ \mu\text{m}$ (cf. Jenniskens et al. 1997), which may affect the determination of the baseline. However, the wavelength coverage of our spectra is insufficient to determine the presence or strength of any such band.

The three spectra are dominated by the deep absorption feature of solid $^{12}\text{CO}_2$ at $\sim 4.27\ \mu\text{m}$, with the solid $^{13}\text{CO}_2$ absorption at $\sim 4.4\ \mu\text{m}$ also present. In the spectra of W33A and AFGL2136 the Br α HI 5–4 recombination line at $4.0523\ \mu\text{m}$ is clearly present, but is very weak, if present, in the spectrum of NGC7538 IRS9. These features were previously identified in ISO spectra by other authors (de Graauw et al. 1996b; Gürtler et al. 1996; Whittet et al. 1996). Also present in the spectrum of W33A and possibly NGC7538 IRS9 is an absorption feature at $\sim 3.93\ \mu\text{m}$, which was originally detected in W33A and identified as solid H_2S (Geballe et al. 1985), or as solid methanol (Allamandola et al. 1992, Dartois et al. 1999). The spectrum of W33A also shows the HI 16–6 and 15–6 lines at $3.8195\ \mu\text{m}$ and $3.9075\ \mu\text{m}$, respectively. Finally, a broad absorption feature between $\sim 4.06\ \mu\text{m}$ and $\sim 4.18\ \mu\text{m}$ is apparent in the spectra of W33A and NGC7538 IRS9, but is not apparent in the spectrum of AFGL2136. This is at the position of the OD stretch of HDO in amorphous H_2O -ice. For comparison, the (scaled) laboratory spectrum of a mixture of $\sim 1\%$ HDO in H_2O -ice at 20 K after annealing at 115 K is plotted superimposed on the spectra of W33A and NGC7538 IRS9 (thick solid lines in the optical depth spectra in Fig. 1). The position and shape of the feature do not vary significantly for concentrations below 5%. The 1% value from the laboratory sample is thus only an order of magnitude indication of the concentration in the astronomical spectra. On the long-wavelength wing of this band, a weaker, sharper feature may be present in the spectra of those two objects. This coincides with the position of the band of HDO in crystalline H_2O -ice. The laboratory spectrum of a mixture of $\sim 0.7\%$ of HDO in crystalline H_2O -ice at 20 K is also plotted for comparison (thin solid lines plotted above the optical depth spectra in Fig. 1). It is stressed that the laboratory spectra shown are *not* the best fits to the observations, and are only given here for comparison to support the proposed identification of the HDO band.

4. Discussion

In view of the wealth of information in the spectra, a detailed analysis will be presented in a later paper. The following discussion is aimed only at establishing the chemical nature of the material producing the $\sim 4.1\ \mu\text{m}$ band.

Of the molecules expected to occur or that have been identified in grain mantles, only two have absorption features at $\sim 4.1\ \mu\text{m}$: HDO and SO_2 . For solid SO_2 , the feature is a weak combination band, but the fundamental asymmetric stretching mode of the molecule occurs at $\sim 7.55\ \mu\text{m}$ (Sandford & Allamandola 1993; Boogert et al. 1997). Boogert et al. (1997) looked for the signature of solid SO_2 at $7.55\ \mu\text{m}$ toward W33A and NGC7538 IRS9. Their results show that solid SO_2 appears to be present toward W33A with a column density of $(1.7 \pm 0.8) \times 10^{17}\ \text{cm}^{-2}$, but only an upper limit of $< 5.5 \times 10^{16}\ \text{cm}^{-2}$ could be placed toward NGC7538 IRS9. Using optical depth spectra a column density, N (molecules/ cm^{-2}), of the absorber can be estimated using $N = (\int \tau_\nu d\nu)/A$, where τ_ν is the optical depth at wavenumber ν (cm^{-1}), and A

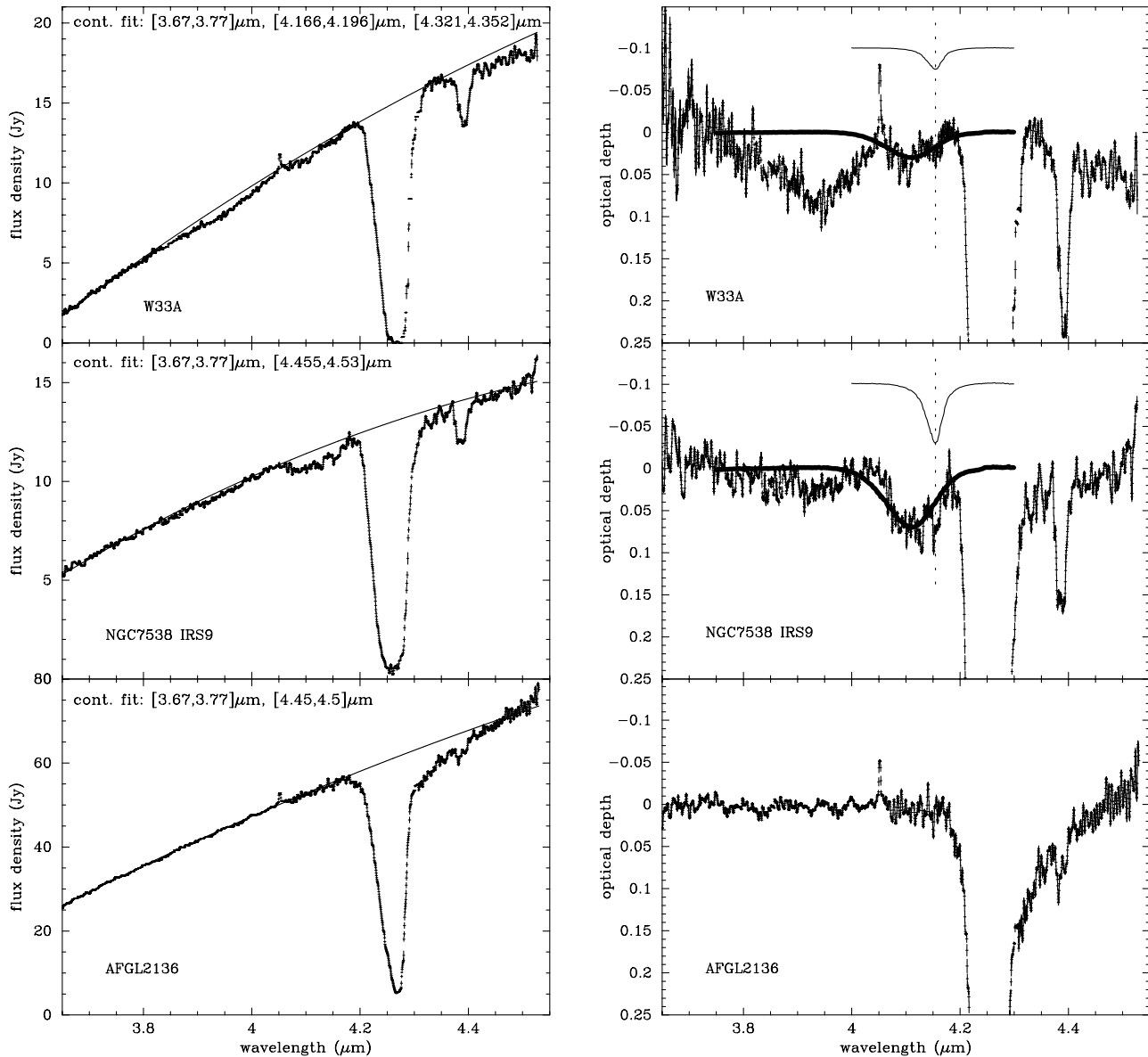


Fig. 1. Spectra of the three targets in Jansky (left-hand side panels) and in optical depth units (right-hand side panels). The continuum fits adopted to derive the spectra in optical depth units are shown as a continuous line overlaid on the observed spectra (left-hand side panels). The regions selected for the continuum fits are indicated over each spectrum. The (barely visible) horizontal errorbars represent the wavelength bins taken to smooth the spectra to a resolution of ~ 2000 . The thick solid lines superimposed on the *optical depth* spectra of W33A and NGC7538 IRS9 correspond to the laboratory spectrum of a mixture of $\sim 1\%$ of HDO in amorphous H_2O -ice. The thin solid lines plotted above the same spectra correspond to a mixture of $\sim 0.7\%$ of HDO in crystalline H_2O -ice (displaced for clarity); the dotted vertical lines mark the peak position of that laboratory band.

(cm/molecule) is the integrated band absorbance (band strength) (e.g. Allamandola et al. 1992). For the SO_2 combination band at $\sim 4.07 \mu\text{m}$, $A = 5 \times 10^{-19}$ cm/molecule (Sandford & Allamandola 1993), which for our spectra leads to a column density of solid SO_2 of $(3.25 \pm 0.03) \times 10^{18} \text{ cm}^{-2}$ for W33A, and $(7.82 \pm 0.03) \times 10^{18} \text{ cm}^{-2}$ for NGC7538 IRS9. These values are one and two orders of magnitude larger than those estimated by Boogert et al.. Solid SO_2 can therefore not be responsible for the absorption feature at $\sim 4.1 \mu\text{m}$ observed toward these objects.

If the $4.1 \mu\text{m}$ absorption features observed towards W33A and NGC7538 IRS9 are due to solid HDO in the grain mantles, then it is possible to estimate the ratio of solid HDO to solid H_2O column densities, $N_s(\text{HDO})/N_s(\text{H}_2\text{O})$, in those lines-of-sight. For the $4.1 \mu\text{m}$ HDO stretch mode, $A = 5.03 \times 10^{-17}$ cm/molecule (Ikawa & Maeda 1968), hence using the optical depth spectra in Fig. 1, we obtain: $N_s(\text{HDO}) = (3.23 \pm 0.03) \times 10^{16} \text{ cm}^{-2}$ for W33A, and $N_s(\text{HDO}) = (7.78 \pm 0.03) \times 10^{16} \text{ cm}^{-2}$ for NGC7538 IRS9. The solid H_2O column densities for these two objects are rather uncertain. The $3.08 \mu\text{m}$ water-ice

band is saturated in the case of W33A ($\tau_{max} > 5.4$), and has a peak optical depth $\tau_{max} = 3.28$ for NGC7538 IRS9 (Willner et al. 1982). Taking $A = 2.0 \times 10^{-16}$ cm/molecule for the $3.08 \mu\text{m}$ water-ice band (d'Hendecourt & Allamandola 1986), and a typical full-width at half-maximum of $\Delta\nu_{1/2} \sim 360 \text{ cm}^{-1}$ (Duley & Smith 1995; Teixeira & Emerson 1999), an estimate of the water-ice column density can be obtained using an approximation of the expression in the previous paragraph: $N \cong \tau_{max} \cdot \Delta\nu_{1/2} / A$. This results in $N_s(\text{H}_2\text{O}) > 9.7 \times 10^{18} \text{ cm}^{-2}$ for W33A, and $N_s(\text{H}_2\text{O}) = 5.9 \times 10^{18} \text{ cm}^{-2}$ for NGC7538 IRS9. The water-ice column density can also be obtained from the $6.0 \mu\text{m}$ OH bend feature (Tielens & Allamandola 1987; Schutte et al. 1996b). The estimates from the $6.0 \mu\text{m}$ band are $N_s(\text{H}_2\text{O}) = 4.2 \times 10^{19} \text{ cm}^{-2}$ for W33A (Allamandola et al. 1992), and $N_s(\text{H}_2\text{O}) = 8.0 \times 10^{18} \text{ cm}^{-2}$ for NGC7538 IRS9 (Schutte et al. 1996b). We conclude that the solid HDO-to- H_2O ratio is in the range of 8×10^{-4} to 3×10^{-3} for W33A, and $\sim 10^{-2}$ for NGC7538 IRS9.

The apparent lack of detection of a feature at $\sim 4.1 \mu\text{m}$ toward AFGL2136 does not preclude an enhancement in the deuteration in the mantles along that line-of-sight. Integration of the optical depth spectrum in Fig. 1 in the same wavelength range as for the other two objects, results in $N_s(\text{HDO}) = (8.0 \pm 0.2) \times 10^{15} \text{ cm}^{-2}$. Because of the uncertainties in the way the spectrum was assembled, and in the determination of the baseline (Sec. 3), this must be regarded as an upper limit. The estimated water-ice column density for AFGL2136 is $N_s(\text{H}_2\text{O}) = 5.0 \times 10^{18} \text{ cm}^{-2}$ (Schutte et al. 1996a). This leads to a ratio $N_s(\text{HDO})/N_s(\text{H}_2\text{O}) \lesssim 2 \times 10^{-3}$, which is within the range of values estimated for W33A.

The $N_s(\text{HDO})/N_s(\text{H}_2\text{O})$ ratios show an enhancement in the deuteration of water in the grain mantles towards at least 2 of the 3 observed objects, of a factor of ~ 50 to ~ 800 relative to the cosmic $[\text{D}]/[\text{H}]$ ratio. These results agree with the lower predictions of the chemical models of dense clouds which include deuterium chemistry and gas-grain interaction (cf. Sec. 1). Moreover, the solid HDO-to- H_2O ratios towards W33A and AFGL2136 are of the same order as the gas phase HDO-to- H_2O ratios observed towards “hot cores” ($(2-6) \times 10^{-4}$; Jacq et al. 1990; Helmich et al. 1996), and only up to a factor of 60 higher towards NGC7538 IRS9. Our HDO/ H_2O ratios are somewhat higher than the $3 \pm 1 \times 10^{-4}$ found in outgassed material (presumably from cometary ices) in Comet C/1996 B2 (Hyakutake) (Bockelée-Morvan et al. 1998), in the sense expected if cometary material has a solar nebula as well as an interstellar component. It would be also interesting to investigate if the HDO/ H_2O ratio correlates with grain (or gas) temperature, but as we cannot estimate the temperature of the HDO containing grains, nor locate them in any particular gas region along the line-of-sight, this is not possible at present. In a future work we will report on the correlations of the amount of HDO with other observed and derived properties of these lines-of-sight, with a view to elucidating the conditions which are favourable for large abundances of HDO ice.

Our results provide support for the assumption that the origin of high levels of deuterium fractionation in “hot cores” is

evaporation of the deuterated species from the grain mantles. These observations provide the first evidence for the presence in the grain mantles of the link that has been missing between observations and models of “hot core” and dark cloud chemistry: deuteration in grain mantles.

Acknowledgements. TCT is very grateful to Dr. Dietmar Kunze for invaluable help with the data reduction whilst at the Les Houches Summer School, Session 70, “Infrared Space Astronomy, Today and Tomorrow”. TCT acknowledges financial support from the School. This work used the NASA Catalog of Infrared Observations (Gezari et al. 1993, 1996, 1997), and the Atomic Line List of the Univ. of Kentucky (P. van Hoof, 1999).

References

- Allamandola L.J., Sandford S.A., Tielens A.G.G.M., Herbst T.M., 1992, *ApJ* 399, 134
 Bergin E.A., Neufeld D.A., Melnick G.J., 1999, *ApJ* 510, L145
 Bockelée-Morvan D., Gautier D., Lis D.C., et al., 1998, *Icarus* 133, 147
 Boogert A.C.A., Schutte W.A., Helmich F.P., Tielens A.G.G.M., Wooden D.H., 1997, *A&A* 317, 929
 Brown P.D., Millar T.J., 1989, *MNRAS* 237, 661
 Dartois E., Schutte W., Geballe T.R., Demyk K., Ehrenfreund P., d'Hendecourt L., 1999, *A&A* 342, L32
 Dring A.R., Linsky J., Murthy J., et al., 1997, *ApJ* 488, 760
 de Graauw T. et al., 1996a, *A&A*, 315, L49
 de Graauw T., Whittet D.C.B., Gerakines P.A., et al., 1996b, *A&A*, 315, L345
 d'Hendecourt L.B., Allamandola L.J., 1986, *A&AS* 64, 453
 Duley W.W., Smith R.G., 1995, *ApJ* 450, 179
 Geballe T.R., Baas F., Greenberg J.M., Schutte W., 1985, *A&A* 146, L6
 Gürtler J., Henning Th., Kömpe C., Pfau W., Krätschmer W., Lemke D., 1996, *A&A* 315, L189
 Helmich F.P., van Dishoeck E.F., Jansen D.J., 1996, *A&A* 313, 657
 Ikawa A.-I., Maeda S., 1968, *Spectrochim. Acta*, 24A, 655
 Jacq T., Walmsley C.M., Henkel C., Baudry A., Mauersberger R., Jewell P.R., 1990, *A&A* 228, 447
 Jenniskens P., Banham S.F., Blake D.F., McCoustra M.R.S., 1997, *J. Chem. Phys.* 107, 1232
 Kessler M.F. et al. 1996, *A&A* 315, L27
 Lacy J.H., Baas F., Allamandola L.J., et al., 1984, *ApJ* 276, 533
 Mayer E., Pletzer R., 1985, *J. Chem. Phys.* 83, 6536
 Millar T.J., Hatchell J., 1998, *Faraday Discuss.* 109, 15
 Millar T.J., Bennett A., Herbst E., 1989, *ApJ* 340, 906
 Rodgers S.D., Millar T.J., 1996, *MNRAS* 280, 1046
 Sandford S.A., Allamandola L.J., 1993, *Icarus* 106, 478
 Schutte W.A., Gerakines P.A., Geballe T.R., van Dishoeck E.F., Greenberg J.M., 1996a, *A&A* 309, 633
 Schutte W.A., Tielens A.G.G.M., Whittet D.C.B., 1996b, *A&A* 315, L333
 Teixeira T.C., Emerson J.P., 1999, *A&A*, submitted
 Tielens A.G.G.M., 1983, *A&A* 119, 177
 Tielens A.G.G.M., Tokunaga A.T., Geballe T.R., Baas F., 1991, *ApJ* 381, 181
 Tielens A.G.G.M., Allamandola L.J., 1987, in: *Physical Processes in Interstellar Clouds*, eds. G.E. Morfill, M. Scholer, Reidel, p. 333
 Whittet D.C.B., Schutte W.A., Tielens A.G.G.M., et al., 1996, *A&A* 315, L357
 Willner S.P., Gillett F.C., Herter T.L., et al., 1982, *ApJ* 253, 174